

# The 3.4 $\mu\text{m}$ absorption of the Titan's stratosphere: contribution of ethane, propane, butane and complex hydrogenated organics

Thibault Cours<sup>a,\*</sup>, Daniel Cordier<sup>a</sup>, Benoît Seignovert<sup>b,a</sup>, Luca Maltagliati<sup>c</sup>, Ludovic Biennier<sup>d</sup>

<sup>a</sup>Université de Reims Champagne Ardenne, CNRS, GSMA UMR 7331, 51097 Reims, France

<sup>b</sup>Jet Propulsion Laboratory, California Institute of Technology, Pasadena, CA 91109, USA

<sup>c</sup>Nature Astronomy, Springer Nature, 4 Crinan Street, N1 9XW London, UK

<sup>d</sup>Institut de Physique de Rennes, UMR CNRS 6251, 35042 Rennes, France

## Abstract

The complex organic chemistry harbored by the atmosphere of Titan has been investigated in depth by Cassini observations. Among them, a series of solar occultations performed by the VIMS instrument throughout the 13 years of Cassini revealed a strong absorption centered at 3.4  $\mu\text{m}$ . Several molecules present in Titan's atmosphere create spectral features in that wavelength region, but their individual contributions are difficult to disentangle. In this work, we quantify the contribution of the various molecular species to the 3.4  $\mu\text{m}$  band using a radiative transfer model. Ethane and propane are a significant component of the band but they are not enough to fit the shape perfectly, then we need something else. Polycyclic Aromatic Hydrocarbons (PAHs) and more complex polyaromatic hydrocarbons like Hydrogenated Amorphous Carbons (HACs) are the most plausible candidates because they are rich in C–H bonds. PAHs signature have already been detected above 900 km, and they are recognized as aerosols particles precursors. High similarities between individual spectra impede abundances determinations.

**Keywords:** Titan, Planets and Satellites, Solar System

**DOI:** [10.1016/j.icarus.2019.113571](https://doi.org/10.1016/j.icarus.2019.113571)

## 1. Introduction

Titan is an extraordinary object among the planets and satellites of the solar system. Its thick atmosphere, mainly composed of nitrogen and methane, harbors a complex photochemistry producing organic compounds that participate to the formation of haze which produces its typical orange/brown color. Due to its unique and exotic properties, Titan's atmosphere remains a very active field of research in investigating the possible origin and main properties (Johnson et al., 2016; Charnay et al., 2014; Newman et al., 2016). Its composition can be modeled by complex chemical network (Krasnopolsky, 2014; Lavvas et al., 2015), but also by laboratory experiments (Bourgalais et al., 2016; Romanzin et al., 2016) to match the observations made by Cassini's instruments (Vinatier et al., 2015; Coustenis et al., 2016; Bellucci et al., 2009). In Bellucci et al. (2009), the authors raised an issue about the CH<sub>4</sub> 3.3  $\mu\text{m}$  band.

In 2006, during Cassini's 10<sup>th</sup> flyby of Titan (T10), Bellucci et al. (2009) observed features in CH<sub>4</sub> 3.3  $\mu\text{m}$  band with the Visible and Infrared Mapping Spectrometer (VIMS). VIMS is an imaging spectrometer onboard the Cassini spacecraft. This instrument is composed of a visible channel (0.3–1.05  $\mu\text{m}$ ) and a infrared channel (0.89–5.1  $\mu\text{m}$ ). The FWHM of the 256 infrared spectral pixels

are in the range 13–20 nm. VIMS can be used in different observation modes corresponding to nadir, limb and occultation geometry. Our study use the latter mode. More details can be found in Maltagliati et al. (2015). Bellucci et al. (2009) tentatively attributed the observed features in CH<sub>4</sub> 3.3  $\mu\text{m}$  band to solid state organic compounds, similar to those observed in the InterStellar Medium (ISM) (Sandford et al., 1991; Pendleton and Allamandola, 2002). However, this interpretation was far to be firm and Bellucci et al. (2009) concluded that precise comparison of their data with laboratory spectrum needed in future work.

Interestingly, a similar feature had been observed by VIMS during a stellar occultations in Saturn's atmosphere (Nicholson et al., 2006; Kim et al., 2012). Continued by Kim et al. (2012), these analysis shown that the optical-depth spectra exhibit a broad peak at 3.36–3.41  $\mu\text{m}$  for the observations obtained at 12 pressure levels between 0.0150 and 0.0018 mbar in the Saturnian atmosphere. Kim et al. (2012), in particular, attributed these 3.4  $\mu\text{m}$  spectral features to the aliphatic C–H stretching bands of solid-state hydrocarbons, such as C<sub>5</sub>H<sub>12</sub>, C<sub>6</sub>H<sub>12</sub>, C<sub>6</sub>H<sub>14</sub> and C<sub>7</sub>H<sub>14</sub>. Kim et al. (2011) reached a similar conclusion for Titan in analyzing the occultation T10.

However, the formation of such organic microcrystals in the atmosphere of Titan is questionable due to thermodynamic arguments (see Sec. 2).

More recently, Maltagliati et al. (2015) analyzed an ex-

\*Corresponding author: [thibaud.cours@univ-reims.fr](mailto:thibaud.cours@univ-reims.fr)

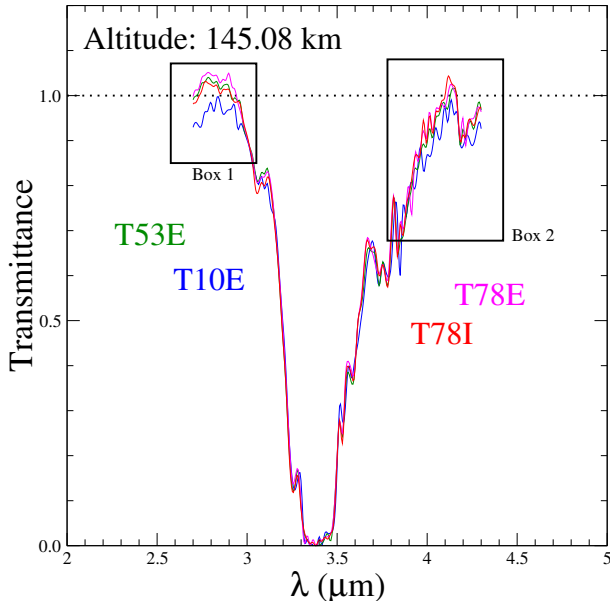


**Fig. 1.** Transmittance curves derived from solar occultations T10E, T53E, T78E and T78I studied by Maltagliati et al. (2015). Altitude interpolations, at 145 km, have been performed to allow easy comparisons. Boxes delineate domains where data are significantly noisy.

tended set of four VIMS solar occultations, performed between January 2006 and September 2011. In Fig. 1, we report an example of transmission data derived from Maltagliati et al. (2015). Spectra have been normalized by a 3<sup>th</sup> order polynomial and data have been interpolated at the altitude of 145 km to allow easy comparisons. This value offers a good compromise: at lower altitudes, the stronger absorptions damp spectral features and at higher altitudes, the absorptions are weak and the spectra are more noisy due to a weaker signal. Deviations between the four curves plotted in Fig. 1 give an idea of transmittance uncertainties, and spatial or temporal variations in Titan’s atmosphere.

In their line-by-line radiative transfer model, Maltagliati et al. (2015) took into account the absorption caused by 9 molecules: CH<sub>4</sub>, CH<sub>3</sub>D, CO, CO<sub>2</sub>, C<sub>2</sub>H<sub>2</sub>, C<sub>2</sub>H<sub>4</sub>, C<sub>2</sub>H<sub>6</sub>, HCN and N<sub>2</sub>. In spite of the level of sophistication of their approach, Maltagliati et al. (2015) found a clear disagreement between the observed absorption in the 3.4 μm band and their computed spectra. It appears then that the atmosphere of Titan is a more efficient absorber than in this model. By comparing the observed residual absorption and the ethane cross sections measured by the Pacific Northwest National Lab (PNNL - Sharpe et al., 2016), and given the lack of C<sub>2</sub>H<sub>6</sub> spectral lines in major databases (HITRAN and GEISA), Maltagliati et al. (2015) interpreted the strong absorption band centered at 3.4 μm as the effect of ethane. These authors also tentatively attribute the narrow absorption at 3.28 μm to the presence of Polycyclic Aromatic Hydrocarbons (PAHs) in the stratosphere. Indeed, a few years before, López-Puertas et al. (2013) identified the presence of these aromatic molecules in Titan’s upper atmosphere around 650 km up

to ~1300 km. Their results rely on the emission near 3.28 μm detected by VIMS.

It is well accepted that a strong absorption at 3.2–3.5 μm is related to the C–H stretching bands, but the C–H bonds can be present in icy hydrocarbons, in simple molecules, in more complex polyaromatic hydrocarbons or in aerosols particles. In this paper, we try to disentangle the problematic attribution of this strong absorption around 3.4 μm. In Fig. 1, transmittances corresponding to box 1 and box 2 are clearly too noisy to allow a clear analysis. In this work, we specifically focus our efforts on the highest absorption spectral range, *i.e.*, between 3.3 and 3.5 μm.

In Sec. 2 we examine, in the light of an advanced thermodynamic model, the possibility of the existence of hydrocarbon ices in the stratosphere of Titan, as proposed by Kim et al. (2011). In Sec. 3 and 4 we revisit the absorption of gases in the 3.4 μm spectral region while in Sec. 5 we discuss the possible presence of PAHs or more complex polyaromatic hydrocarbons like Hydrogenated Amorphous Carbons (HACs). In Sec. 6 and 7, we further discuss these issues and present our conclusions.

## 2. Solid-Vapor equilibria in Titan’s stratosphere

**Table 1:** Triple points coordinates for the sample of hydrocarbon species considered by Kim et al. (2011). The temperatures have all been taken in the NIST database<sup>†</sup>, for CH<sub>3</sub>CN, C<sub>5</sub>H<sub>12</sub> and C<sub>6</sub>H<sub>12</sub>. The pressures are not available in this database, we then estimated their values by using their Antoine’s equation at the triple point temperature.

Species	Chemical formula	$T_{\text{triple}}$ (K)	$P_{\text{triple}}$ (bar)
Ethane	C <sub>2</sub> H <sub>6</sub>	91.0	$1.1 \cdot 10^{-5}$
Methane	CH <sub>4</sub>	90.7	$1.2 \cdot 10^{-1}$
Methylcyanide	CH <sub>3</sub> CN	229.3	$2.2 \cdot 10^{-3*}$
Pentane	C <sub>5</sub> H <sub>12</sub>	143.5	$3.9 \cdot 10^{-7*}$
Cyclohexane	C <sub>6</sub> H <sub>12</sub>	279.7	$5.3 \cdot 10^{-2*}$

<sup>†</sup> [webbook.nist.gov/chemistry](http://webbook.nist.gov/chemistry)

\* Our estimation

An explanation for the nature of Titan’s 3.4 μm absorption was put forward by Kim et al. (2011) who could reproduce the VIMS solar occultations by using hydrocarbon ices like C<sub>2</sub>H<sub>6</sub>, CH<sub>4</sub>, CH<sub>3</sub>CN, C<sub>5</sub>H<sub>12</sub> and C<sub>6</sub>H<sub>12</sub> ices. However, the real existence of such ices in the stratosphere of Titan needs to be discussed. Indeed, as mentioned by Kim et al. (2011), above 130 km (the lowest altitude explored by these authors) the temperature remains in 160–190 K interval while the pressure decreases below  $5 \cdot 10^{-3}$  bar. A look at Table 1, in which we have gathered the triple points coordinates of involved species, shows that at least C<sub>2</sub>H<sub>6</sub>, CH<sub>4</sub> and C<sub>5</sub>H<sub>12</sub> should not be in solid form at these relatively high temperatures.

In order to investigate more deeply the existence of these ices, we introduce two quantities, the first is:

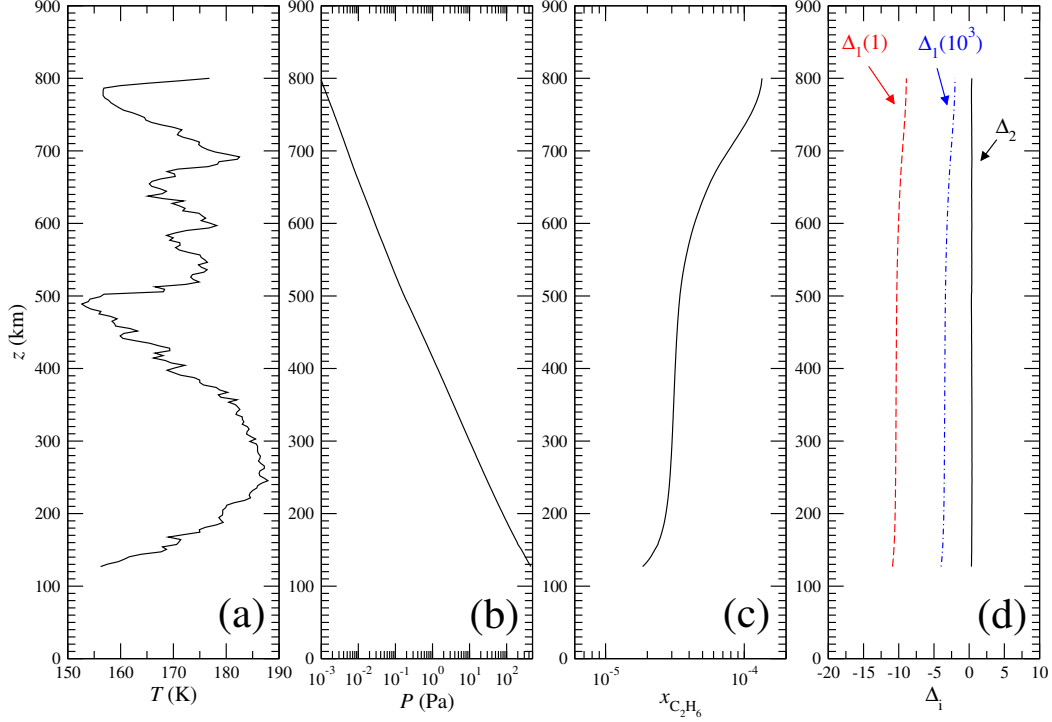


**Fig. 2.** Panels (a) and (b) stand respectively for the temperature and pressure profiles, provided by HASI instruments, between the altitudes 127 km and 800 km in the atmosphere of Titan (Fulchignoni et al., 2005). Panel (c) represents the molar fraction of ethane as computed by Lavvas et al. (2008a,b). In panel (d) the thermodynamic quantities  $\Delta_1$  and  $\Delta_2$  (defined in the text by Eq. (1) and Eq. (2)) for ethane. We recall that  $\Delta_1$  and  $\Delta_2$  correspond respectively to the chemical potential, of a given species, in the gas phase and in the solid phase, the coexistence of both is reached when  $\Delta_1 = \Delta_2$  (see Eq. (3)).  $\Delta_1(1)$  corresponds to the abundances found by Lavvas *et al.*'s while  $\Delta_1(10^3)$  has been obtained by multiplying the mole fraction  $x_{C_2H_6}$  by  $10^3$ .

$$\Delta_{1,i} = \ln(\Gamma_i^{\text{vap}} y_i) \quad (1)$$

where  $y_i$  is the mole fraction of the compound  $i$  at equilibrium, in the vapor, and  $\Gamma_i^{\text{vap}}$  is the activity coefficient of the considered species. The second introduced term is written as:

$$\Delta_{2,i} = -\frac{\Delta H_{i,m}}{RT_{i,m}} \left( \frac{T_{i,m}}{T} - 1 \right) \quad (2)$$

The thermodynamic equilibrium between the species  $i$  in the vapor, and its icy counterpart, is reached when the equation:

$$\Delta_{1,i} = \Delta_{2,i} \quad (3)$$

is satisfied (Poling et al., 2007). Eq. (3) corresponds to a thermodynamic equilibrium between the considered organic ice  $i$  and the vapor – Eq. (3) is an equality of chemical potential. The activity coefficient  $\Gamma_i^{\text{vap}}$  is given by the Perturbed-Chain Statistical Associating Fluid Theory (PC-SAFT). Originally proposed by Gross and Sadowski (2001), PC-SAFT is now widely employed in the chemical engineering community, due to its very good performances. This theory has been successfully employed in several recent studies of Titan to model liquid-vapor and solid-liquid equilibria (Tan et al., 2013; Luspai-Kuti et al., 2015; Tan et al., 2015; Cordier et al., 2016; Cordier, 2016).

In Eq. (1) the activity coefficient  $\Gamma_i^{\text{vap}}$  quantifies the *degree of ideality* of the considered gas mixture. When  $\Gamma_i^{\text{vap}} \sim 1$  the system has an ideal behavior, *i.e.*, all the molecules of the same species and those of different species interact with the same intensity. In our context, for all the molecules listed in Table 1, we found the  $\Gamma_i^{\text{vap}}$ 's very close to unity, whatever the altitude. This indicates an ideal behavior of the gases, which is not a surprise at densities provided by HASI measurements (Fulchignoni et al., 2005). Practically, this means that Eq. (3) can be satisfied only if  $\Delta_{2,i}$  is negative, meaning that the molar fraction  $y_i$  has to be smaller than unity. In the case of ethane,  $\Delta_{2,i}$  remains slightly larger than zero (see Fig. 2.d), then, in the conditions of pressure and temperature in the Titan's stratosphere, according to the present model,  $C_2H_6$  can never form solid particles. For the other species, even if  $\Delta_{2,i} < 0$ , the measured or estimated values of their mole fractions are order of magnitude too small for Eq. (3) to be satisfied. For instance, concerning  $CH_3CN$ , (Lara et al., 1996, see their Fig. 10 p279) reported abundances, derived from ground-based millimeter-wave observations (Bézard et al., 1993), between roughly  $10^{-9}$  and  $10^{-7}$  in molar fraction, while Lavvas et al. (2008a,b) computed values around  $10^{-8}$ . Our calculations show that even in the most favorable case (*i.e.*, when the abundances of  $CH_3CN$  is taken equal to  $10^{-7}$ ) the term  $\Delta_{1,i}$  is more than ten orders of magnitude smaller than the typical value of  $\Delta_{2,i}$  in stratospheric conditions. As a consequence, we conclude that

the compounds proposed by Kim et al. (2011) cannot exhibit solid-vapor equilibria in the stratosphere of Titan. The only possibility remaining is the presence of these icy hydrocarbon aerosols in a non-equilibrium state, but such a situation seems unlikely.

### 3. Radiative transfer modeling of the 3.4 $\mu\text{m}$ absorption

In order to simulate the properties of the flux of photons that emerges from the Titan’s atmosphere during a solar occultation, we have built a simple radiative transfer model. On one hand, the structure of the atmosphere is represented by a set of concentric spherical shells; on the other hand, the solar radiations are assumed to follow a straight optical path through the atmosphere. The refraction is neglected in our entire approach, this approximation is relevant due to the low density probed in these explored regions. For a given altitude  $z$ , the transmittance  $T(\lambda, z)$  of the atmosphere at the wavelength  $\lambda$  is estimated using:

$$T(\lambda, z) = \exp \left( - \sum_{i,j,k} N_j x_{i,j} \sigma_{i,k} l_j \right) \quad (4)$$

where the indexes  $i$ ,  $j$  and  $k$  denote respectively the chemical species, the atmospheric layers and the spectral lines. The cross-sections are  $\sigma_{i,k}$ ,  $N_j$  represents the total number of molecules (per units of volume) in layer  $j$ , while  $x_{i,j}$  is the molar fraction of species  $i$  in the same layer. Finally  $l_j$  stands for the distance travelled by photons in the layer  $j$  (see Fig. 3). Doing several tests on the number of layers, we found  $N_{\text{layers}} = 70$  to be a sufficient total number of shells, linearly distributed between the ground and a maximum altitude of 700 km. The pressure and temperature profiles come from HASI measurements (Fulchignoni et al., 2005). The cross-section  $\sigma_{i,k}$  (in  $\text{cm}^2/\text{molecule}$ ) are written as:

$$\sigma_{i,k}(\tilde{\nu}) = I_{i,k}(\tilde{\nu}_{i,k}) f(\tilde{\nu} - \tilde{\nu}_{i,k}) \quad (5)$$

where  $f$  is a Voigt profile,  $\tilde{\nu}$  and  $\tilde{\nu}_{i,k}$  are respectively the wavenumber (in  $\text{cm}^{-1}$ ) and the spectral line  $k$  wavenumber of the chemical species  $i$ ,  $I_{i,k}$  are the intensities (in  $\text{cm}/\text{molecule}$ ) of the spectral line  $k$  of the chemical species  $i$ . In the cases where high resolution spectral data are available, the cross-section  $\sigma_{i,k}$  are computed using  $k$ -correlated coefficient method (Arking and Grossman, 1972; Chou and Arking, 1980; Fu and Liou, 1992). When only low resolution spectral data are available in the literature or when the lines are wider than the spectral resolution of VIMS (16–20 nm), the  $k$ -correlated coefficient method is not necessary to compute cross-section and therefore a Gauss profile has been proved to be sufficient.

Our initial composition is based on the one published by Maltagliati et al. (2015) and include the following

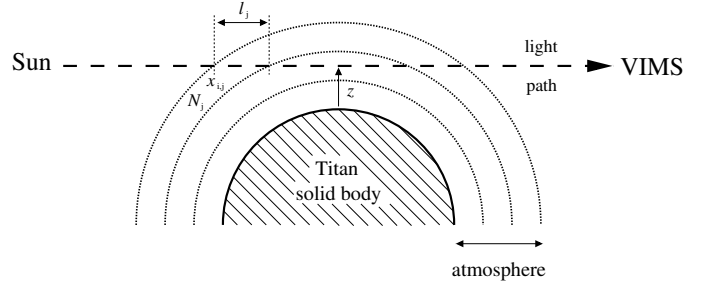


**Fig. 3.** A schematic representation of our *onion-skin* radiative transfer model, used in this paper and suitable for the analysis of Titan’s solar occultations data published by Maltagliati et al. (2015). In the text, the term *altitude* refers to the parameter called  $z$  in this figure. After tests with different numbers of layers, a total number  $N_{\text{layers}} = 70$  of atmospheric layers was found sufficient to describe the atmosphere. Layers have been linearly distributed between the ground and 700 km.

molecules:  $\text{CH}_4$ ,  $\text{CH}_3\text{D}$ ,  $\text{CO}$ ,  $\text{C}_2\text{H}_2$ ,  $\text{C}_2\text{H}_4$ ,  $\text{C}_2\text{H}_6$ ,  $\text{H}_2\text{O}$ ,  $\text{C}_6\text{H}_6$  and  $\text{HCN}$ . In this entire paper, we adopt this list of species as our First Guess composition (hereafter FG composition), the influence of other compounds will be made by comparing what it is obtained using this FG composition. Nitrogen is voluntarily omitted since it is extremely poor absorbent in the domain of interest. Moreover, the collision-induced effects are negligible within the band 3.3–3.5  $\mu\text{m}$ . The  $\text{CH}_4$ ,  $\text{C}_2\text{H}_2$ ,  $\text{C}_2\text{H}_4$ ,  $\text{C}_2\text{H}_6$ ,  $\text{C}_6\text{H}_6$  and  $\text{HCN}$  vertical mixing ratio profiles come from photochemical models developed by Krasnopolsky (2014). The abundance of deuterated methane ( $\text{CH}_3\text{D}$ ) with respect to the methane has been kept constant with a  $\text{CH}_3\text{D}/\text{CH}_4$  ratio of about  $5.3 \cdot 10^{-4}$  (Bézard et al., 2007). Concerning water, we performed tests including molar fractions corresponding to the highest value given by Coustenis et al. (1998). Finally, the abundance of  $\text{CO}$  has been taken from Flasar et al. (2005).

The spectral data of  $\text{CO}$ ,  $\text{C}_2\text{H}_2$ ,  $\text{H}_2\text{O}$  and  $\text{HCN}$  were mainly taken in HITRAN<sup>1</sup> (Rothman et al., 2013) and GEISA<sup>2</sup> (Jacquinot-Husson et al., 2008). For  $\text{CH}_4$ ,  $\text{CH}_3\text{D}$  and  $\text{C}_2\text{H}_4$  we used the up-to-date theoretical line lists computed by Rey et al. (2016) and available at the Theoretical Reims-Tomsk Spectral database<sup>3</sup>.

For benzene, due to the lack of data in these database, we performed *ab initio* computations of its absorption frequencies and their respective intensities. Based on the MP2/6-311G\*\* level of the theory, developed by Møller and Plesset (1934), we obtained frequencies, which were scaled by 0.95, according to that is the recommended in such a situation. The only none zero intensities near the 3.4  $\mu\text{m}$  band are for the frequencies  $3064.0917 \text{ cm}^{-1}$  (3.26  $\mu\text{m}$ ) and  $3064.0949 \text{ cm}^{-1}$  (3.26  $\mu\text{m}$ ) (including the scaling factor of 0.95) corresponding to two C–H asymmetric stretching normal modes. The intensities were found quite low with values of 32.63 km/mole for both transitions. Considering

<sup>1</sup>hitran.org

<sup>2</sup>www.pole-ether.fr/geisa

<sup>3</sup>theorets.tsu.ru



the vertical profile of  $C_6H_6$ , we find that the benzene is a minor absorber around  $3.26\ \mu m$ .

Maltagliati et al. (2015) selected a set of four occultations data, T10 Egress (T10E), T53 Egress (T53E), T78 Egress (T78E) and T78 Ingress (T78I) acquired during three flybys, T10, T53 and T78 respectively. For each occultation, the altitude ranges between  $\sim 50\ km$  and  $\sim 690\ km$ . We provide, in supplementary material, four cube's name lists used in our analysis, one name list by occultation. The name lists are in Excel cvs format and can be downloaded from the pds-rings site<sup>4</sup>. For all these occultations, the retrieved transmittance curves, at a given altitude, are extremely similar (see for instance Fig. 11 of Maltagliati et al., 2015). In order to facilitate comparison between our theoretical output, and observational determinations, we have chosen the Ingress occultation T78 (T78I) as a typical case. We also selected the altitude of  $145\ km$  because it offers a good compromise between high altitudes data for which the transmittance curves are pretty flat, and low altitudes measurements presenting a global strong absorption that masks or damps spectral features.

A first model-observation comparison can be seen in Fig. 4, the disagreement is clear, particularly around  $3.4\ \mu m$  our domain of interest. This nicely confirms the findings by Maltagliati et al. (2015).

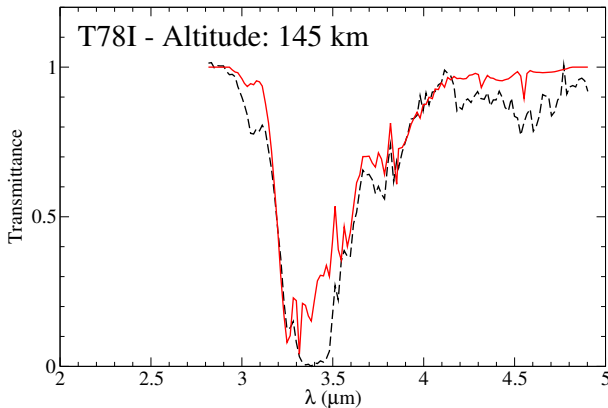


**Fig. 4.** Comparison between observed transmittance (dashed line) acquired during occultation T78I at the altitude of  $145\ km$  (Maltagliati et al., 2015), and the computed transmittance due to our FG composition: with only  $CH_4$ ,  $CH_3D$ ,  $CO$ ,  $C_2H_2$ ,  $C_2H_4$ ,  $C_2H_6$ ,  $H_2O$ ,  $C_6H_6$  and  $HCN$ . For  $C_2H_6$ , only spectral lines provided by HITRAN have been taken into account.

#### 4. The possible absorption of ethane, propane and butane around $3.4\ \mu m$

##### 4.1. Ethane

As already mentioned, the C–H stretching bands produce a strong absorption at  $3.2\text{--}3.5\ \mu m$ , this is why any compound containing one or several C–H bonds can potentially contribute to the observed  $3.4\ \mu m$  absorption. In

this context, ethane, quantitatively the main product of Titan's photochemistry (Lavvas et al., 2008a,b; Krasnopolsky, 2014), should be the object of our first intentions. The presence of ethane in the Titan's atmosphere is firmly established by previous observations, *e.g.*, it has been detected by Cassini's instruments: UVIS (Koskinen et al., 2011), INMS (Cui et al., 2009) and CIRS (Vinatier et al., 2010). Unfortunately, in HITRAN and GEISA databases, ethane spectral lines in the band of interest are pretty scarce. Surprisingly, the absorption spectrum of the C–H stretching region of ethane, measured by Pine and Lafferty (1982) (hereafter PL82) at  $T = 119\ K$ , is not available in these compilations. Then, we included the  $\sim 3000$  lines provided by PL82 data in our model; 1614 entries specify wavenumbers, intensities and the lower state energies whereas for 1426 other entries the lower state energy is not available. Thus, in the latter case, we have neglected the temperature corrections of the intensities. The contribution to the absorption around  $3.4\ \mu m$ , of ethane alone, is plotted in Fig. 5(a).

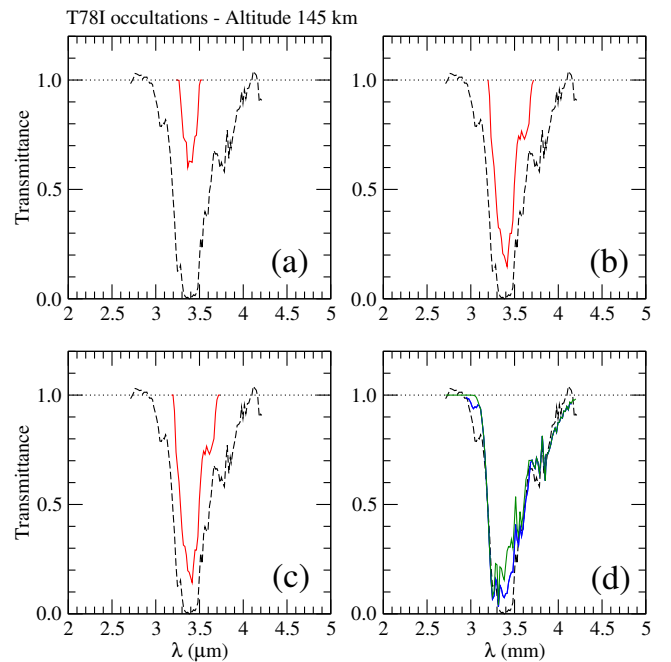


**Fig. 5.** Comparison between simulated transmittances and VIMS for the T78I occultation data (Maltagliati et al., 2015). Observational data are in dashed line, the altitude is  $145\ km$ . This figure shows the transmittance of  $C_2H_6$  using: (a) only Pine and Lafferty (1982) spectral lines (red), (b) only pseudo-lines lists based on the cross-section measurements (Harrison et al., 2010) (red), (c) the combination of PL82 and H10 spectral data (red), (d) the combination of our FG composition model with PL82 and H10 (blue), the absorption computed with our FG composition is also plotted for comparison (green solid line).

Unfortunately, Pine and Lafferty (1982) did not include ethane PQ-branches which should have a non-negligible contribution in the domaine of interest. To tackle the issue, we used an empirical pseudo-line list based on the cross-section measurements developed by Harrison et al. (2010) (hereafter H10 dataset) and freely available on the

<sup>4</sup>[pds-rings.seti.org/cassini/vims](http://pds-rings.seti.org/cassini/vims)

web<sup>5</sup>. Compared to the absorption obtained with PL82 spectral lines, the effect of ethane is significantly enhanced by the use of this more comprehensive list (Fig. 5.b). If both, the PL82 and H10 spectral data, are simultaneously included in our model (Fig. 5.c), the actual effect of PL82 is not noticeable. Finally, if we merge PL82 and H10 spectral lines sets, with those employed for our FG composition model, the disagreement with Cassini/VIMS observations is considerably reduced (Fig. 5.d). This clearly demonstrates the prominent role of ethane, as an absorber, at wavelengths around 3.4  $\mu\text{m}$ . Nonetheless, the simulated transmittance remains significantly above the observed one. This fact suggests the presence of other absorbers, possibility which we discuss further in next paragraphs.

#### 4.2. Propane

According to photochemical models (Lavvas et al., 2008a,b; Krasnopolsky, 2014), propane should also be produced in Titan's upper-atmosphere. This  $\text{C}_3$  hydrocarbon has been detected by several Cassini's instruments: Nixon et al. (2013) determined its mixing ratio using CIRS, while Cui et al. (2009) and Magee et al. (2009) retrieved abundances from INMS measurements. Similarly to the ethane case, HITRAN and GEISA are very poor in spectral data around 3.4  $\mu\text{m}$  for this molecule. Then, we used the propane pseudo-lines list based on the cross-section measurements of Harrison and Bernath (2010) (freely available on the web<sup>6</sup>). Taking into account the propane abundance profile predicted by Krasnopolsky (2014), we have estimated the corresponding absorption in our domain of interest: in Fig. 6 we have displayed the absorption of propane alone a), the effect of this molecule is combined with that of our FG composition sample b), clearly the contribution of propane is comparable to that of ethane, even is propane is approximately one order of magnitude less abundant than ethane. In fact, due to its larger numbers of C-H, propane is an absorber roughly one order of magnitude more efficient than ethane.

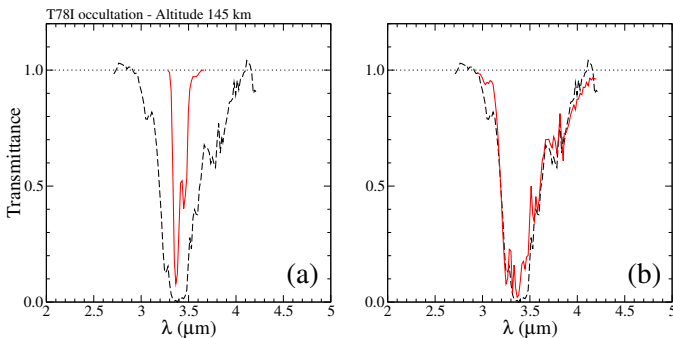


**Fig. 6.** Occultation T8I at 145 km (observed transmittance in dash line): (a) Absorption due to propane alone, (b) computed absorption using our FG composition complemented by propane (ethane is not taken into account).

#### 4.3. Butane

Butane has not yet been detected, in the atmosphere of Titan. The presence of butane is predicted by photochemical models (Krasnopolsky, 2009, 2010, 2014). The quantity of butane should be lower than what it is measured and computed for propane. Available models indicate a butane mixing ratio about four order of magnitude smaller than what Krasnopolsky (2014) obtained for propane. Since no data concerning butane were found in HITRAN and GEISA databases, we used cross-sections provided by the NIST<sup>7</sup>. According to this approach and taking vertical profile provided by Krasnopolsky (2014), we have checked that butane has no detectable influence on the 3.4  $\mu\text{m}$  atmospheric transmittance.

#### 4.4. Conclusion about ethane, propane, butane and others linear hydrocarbon

We have summarized our simulations results in Fig. 7, clearly the addition of propane to our set of considered gaseous species reduced the disagreement between theoretical output and solar occultation data. However, the situation is far from satisfactory, and there is room for other efficient absorbers around 3.4  $\mu\text{m}$ . It is likely that other larger linear hydrocarbons are present in the atmosphere, but they are not yet retrievable from the occultation data. Moreover, their molar fractions could be very small in comparison with the molar fraction of butane. Thus, no additional linear hydrocarbon larger than butane was considered in our model.

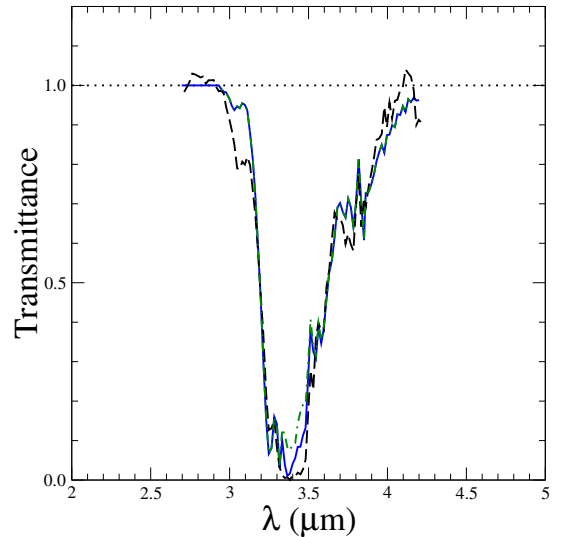


**Fig. 7.** Dashed line: T8I observations, dot-dashed line: our computation taking into account gases of our FG composition and ethane (including pseudo-lines and PL82 data), solid line: the same simulation including propane pseudo-lines list based on the cross-section measurements of Harrison and Bernath (2010).

<sup>5</sup>mark4sun.jpl.nasa.gov/pseudo.html

<sup>6</sup>mark4sun.jpl.nasa.gov/pseudo.html

<sup>7</sup>webbook.nist.gov

## 5. The absorption due to Polycyclic Aromatic Hydrocarbons and Hydrogenated Amorphous Carbons

As mentioned in the introduction, PAHs or more complex polyaromatic hydrocarbons like HACs (Dartois et al., 2004, 2005, 2007), considered as organic compounds in solid state, are detected in the ISM (Sandford et al., 1991; Pendleton and Allamandola, 2002). For instance in Dartois et al. (2004) the features observed in the ISM spectra fitted very well with those observed in spectra of HACs produced in laboratory (Dartois et al., 2004, 2005). Furthermore, PAHs are detected on the Iapetus' and Phoebe's surface (Cruikshank et al., 2008), in micro-meteorites in Antarctic (Becker et al., 1997) and in the meteorite Allende (Becker and Bunch, 1997). Observations of comets reveal the presence of PAHs (Li, 2009) and in addition they were considered in Titan's upper atmosphere to explain an unidentified emission at 3.3  $\mu\text{m}$  (Dinelli et al., 2013; López-Puertas et al., 2013). According to Bellucci et al. (2009) for Titan's atmosphere and Dartois et al. (2004, 2005, 2007); Sandford et al. (1991); Pendleton and Allamandola (2002) for the ISM, the features observed between 3.38 and 3.48  $\mu\text{m}$  are due to the symmetric and asymmetric stretching of the C–H bond in  $-\text{CH}_2$  and  $-\text{CH}_3$  groups of the aliphatic chains. Likewise the features around 3.3  $\mu\text{m}$  are signatures of stretching of aromatic C–H bond (Bellucci et al., 2009; Dartois et al., 2004, 2005, 2007). These latter signatures emphasize the presence of aromatic compounds like PAHs and the signatures at 3.38 and 3.48  $\mu\text{m}$  together with the signatures of aromatic C–H stretching show the presence of complex particles containing aromatic cycles and aliphatic chains as it would expect in HACs. In Dartois et al. (2005), possible structures of HACs compatible with the ISM spectra were simulated with a neuronal network simulation: The resulting structure shows aromatic cycles and aliphatic chains as expected.

Thus, to clarify the observed transmission in the 3.3–3.5  $\mu\text{m}$  spectral region we considered PAHs and HACs compounds in our model.

### 5.1. Polycyclic Aromatic Hydrocarbons

The information on PAHs's transition intensities come from the NASA Ames PAHs IR Spectroscopic Database<sup>8</sup>. In our calculations the line widths were fixed to a reasonable value of 30  $\text{cm}^{-1}$ . This value is approximately comparable to the different values used for HACs (Dartois et al., 2007). We introduce a correction factor  $\alpha_{i,k}$  for the intensities  $I_{i,k}$ , with the same meaning for index  $i$  and  $k$  than the index in Eq. (4), to account for two sources of uncertainty: (1) the temperature dependence of the intensities  $I_{i,k}$ , (2) the uncertainties on the  $I_{i,k}$ 's themselves. Indeed, the spectral data provided by the Ames Database are valid for a temperature of 296 K while the actual temperature in Titan's stratosphere is substantially lower (see

for instance Fig. 5.a). In the spectral window of interest (*i.e.*, 2700–3570  $\text{cm}^{-1}$ ), for the 716 species reported in the Ames database, we counted a total of 11,307 calculated spectral lines against only 127 coming from an experimental determination. Even if some overlaps are present, we see that the majority of available spectral data are calculated theoretically. This rises the question of the degree of confidence that can be placed in these computed data. In this context, we have searched for theoretical and experimental spectral lines that coincide in terms of wavelength, adopting a given tolerance, respectively: 1  $\text{cm}^{-1}$ , 2  $\text{cm}^{-1}$  and 3  $\text{cm}^{-1}$ . This way, we identified 52 lines that correspond to both theoretical and laboratory determinations with a tolerance of 1  $\text{cm}^{-1}$ , 108 when is increased to 2  $\text{cm}^{-1}$  and 144 when the tolerance is increased to 3  $\text{cm}^{-1}$ . Consequently, we formed the log ratio  $I_{\text{th}}/I_{\text{exp}}$  for each identified couple of lines, with  $I_{\text{th}}$  the theoretical intensity and  $I_{\text{exp}}$  the corresponding laboratory measurement. The histograms of log ratio  $I_{\text{th}}/I_{\text{exp}}$  values is plotted in Fig. 8. This figure shows clearly that the theoretical intensities tend to be underestimated, compared to their experimental counterparts, by a factor up to two orders of magnitude. Then, these results motivated our introduction of a factor  $\alpha_{i,k}$  that represents the uncertainties that affect the spectral lines intensities available in the Ames database. In this manner, the intensity  $I_{i,k}$  in Eq. (5) is replaced by the product  $\alpha_{i,k}I_{i,k}$ . Finally, if we combine Eq. (4) with Eq. (5), the product  $\beta_{i,j,k} = x_{i,j}\alpha_{i,k}$ , with the same meaning for index  $j$  than the index in Eq. (4), appears in the expression of the transmission. In first approach, we considered that the correction factors  $\alpha_{i,k}$  are independent of the spectral lines. Therefore,  $\beta_{i,j,k} = x_{i,j}\alpha_{i,k}$  becomes  $\beta_{i,j} = x_{i,j}\alpha_i$ . We took 118 neutral and charged PAHs in the Ames database. We have chosen PAHs with less than 100 carbon atoms, free of Fe, Mg, Si (not relevant for Titan's atmosphere) and for which the intensities are significant in the 3.3–3.5  $\mu\text{m}$  band.

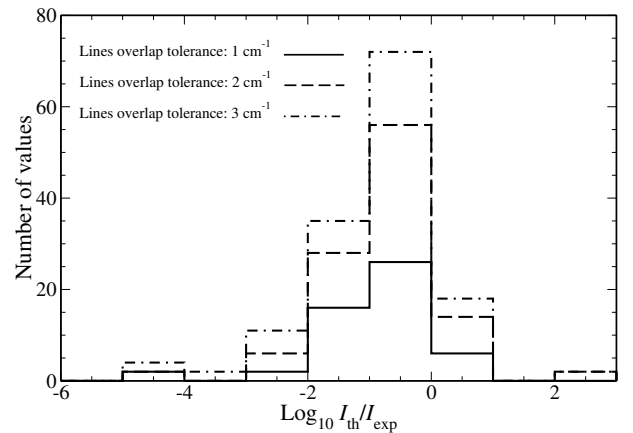


**Fig. 8.** Histograms of the log ratios  $I_{\text{th}}/I_{\text{exp}}$  for the Ames database PAHs for which theoretical and experimental spectral lines features determinations are available. We have considered 3 cases: (1) the wavelengths of theoretical and experimental match with a maximum tolerance of 1  $\text{cm}^{-1}$ , (2) the same with 2  $\text{cm}^{-1}$  and finally 3  $\text{cm}^{-1}$ .

<sup>8</sup>[astrochem.org/pahdb](http://astrochem.org/pahdb)

### 5.2. Hydrogenated Amorphous Carbons

The HACs (sometimes noted a-C:H or a-C:H:N if the HACs contain nitrogen), are considered as smallest haze particle and precursor of more complex haze particle (Lavas et al., 2011; Müller-Wodarg et al., 2013, p.304). In Dartois et al. (2004, 2005, 2007) no identified structure was given but just different vibration modes together with their vibrational frequencies or wavelengths. Analyzing the spectrum of the galaxy named IRAS 08572+3915, Dartois et al. (2007) fitted the intensities, wavelengths and widths of the lines for these vibration modes. Then, we use spectrum parameters given in Table 1 of Dartois et al. (2007). We do not consider HACs with nitrogen (a-C:H:N) because the vibrational modes containing N are not present in 3.3–3.5  $\mu\text{m}$  band (Dartois et al., 2005). As with PAHs, we also introduce a correction factor  $\alpha_{i,k}$  on the intensities  $I_{i,k}$ , with the same meaning for index  $i$  and  $k$  than the index in Eq. (4), taking into account for an uncertainty source: the temperature dependence of the intensities  $I_{i,k}$ . Indeed, the intensities coming from the study of IRAS 08572+3915 spectrum the temperature must be different than that in Titan’s stratosphere. In Dartois et al. (2007) no distinction was made between the different HACs but just between the vibration modes. Consequently, in our model for HACs we omit index  $i$ . Thus, our correction factor  $\alpha_{i,k}$  becomes  $\alpha_k$  and the intensities are  $I_k$ . In first approach, as with PAHs, the correction factors  $\alpha_k$  are independent of the spectral lines. Consequently, we define a product  $\beta_j = x_j \alpha$ .

### 5.3. Results

For PAHs,  $x_{i,j}$  is the molar fraction of PAHs number  $i$  with respect to the  $\text{C}_6\text{H}_6$  abundance profile in layer  $j$ . As a first approximation, the vertical profile of this molar fraction of PAHs number  $i$  vs the  $\text{C}_6\text{H}_6$  (used as proxy) abundance and the vertical profile of the molar fraction of HACs were kept constant. Thus for PAHs and HACs respectively,  $\beta_{i,j} = x_{i,j} \alpha_i$  turns into  $\beta_i = x_i \alpha_i$  and  $\beta_j = x_j \alpha$  turns into  $\beta = x \alpha$ . Considering the uncertainties on PAHs and HACs intensities, we have fitted, respectively, the product  $\beta_i = x_i \alpha_i$  and not  $x_i$  alone, and  $\beta = x \alpha$  and not  $x$ , to get the best fit to occultation data. However, the resulting values do not provide information about the actual abundances of these PAHs and HACs because the problem is degenerated: the correction coefficient to apply remains unknown. Taking into account the log ratio  $I_{\text{th}}/I_{\text{exp}}$  and according to the PAHs number  $i$ , we obtain as best fit for  $\beta_i$ , values in the range of  $4.75 \cdot 10^{-4}$ – $3.32 \times$  molar fraction of  $\text{C}_6\text{H}_6$ . Concerning the HACs, the best fit for  $\beta$  is found for the value  $10^{-7}$ .

Fig. 9 shows that the combination of all gases, plus the 118 PAHs and HACs allow a satisfactory modelization of the observed transmittance at 145 km.

## 6. Discussion

Observations of Saturn’s stratospheric auroral regions (Guerlet et al., 2015) seem to underline the remarks made

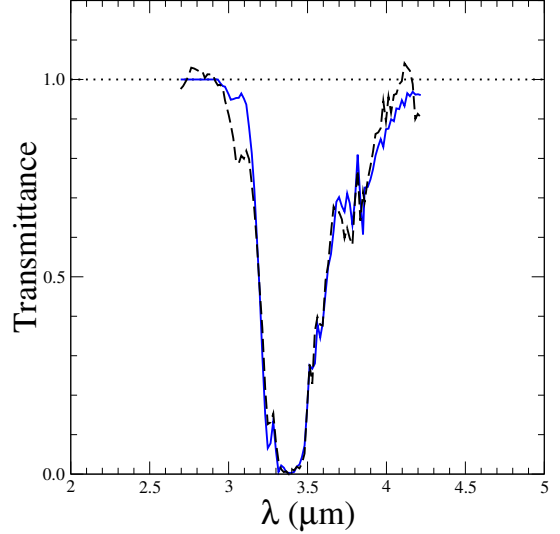


**Fig. 9.** Computed transmittance (solid line) at 145 km during occultation T78I (observed transmittance in dash line), the radiative transfer model takes into account all studied gases plus the best fit of 118 PAHs (from NASA Ames database) and HACs (from Dartois et al., 2007).

on the features observed in Titan’s atmosphere. Indeed, spectral signatures of benzene and aerosols in the range 680–900  $\text{cm}^{-1}$  and 1360–1440  $\text{cm}^{-1}$  have been observed with CIRS on board Cassini, around the 80°S. In particular, vibrational modes in aliphatic and aromatic hydrocarbons were observed revealing the presence of PAHs or HACs in stratosphere of Saturn (Guerlet et al., 2015). Moreover, as mentioned, VIMS observations of Procyon’s occultation through Saturn’s atmosphere around the 55°N, reported by Nicholson et al. (2006) and discussed by Bellucci et al. (2009), show similar features in the 3.4  $\mu\text{m}$  band to those observed in our study. Nevertheless, the observations reveal slight differences with the Titan’s 3.4  $\mu\text{m}$  band spectra. But these differences could be due to a lower amount of nitrogen compounds in Saturn’s atmosphere (Bellucci et al., 2009). Thus, the PAHs and HACs in Titan’s atmosphere could be slightly different from those in Saturn’s atmosphere.

Our study of 3.4  $\mu\text{m}$  band observed by solar occultation at 145 km of altitude suggests the presence of aromatic molecules like PAHs and more complex like HACs at low altitudes. Some insights can be gained by examining the results from laboratory experiments. Dartois et al. (2004, 2005) synthesized HACs (called a-C:H in these references) by ultraviolet photolysis of methane (Dartois et al., 2004) and other hydrocarbons and nitrogen compounds to form a-C:H:N compounds (Dartois et al., 2005) by UV radiation with wavelengths shorter than 120 nm in the EUV domain. Then, they made spectral Infra-Red (IR) analysis of the residues. The aim of these previous studies was to explain the spectral features observed in the ISM. Due to the presence of methane, others hydrocarbons and nitrogen compounds as well as the ultraviolet radiation in EUV domain going down to 600 km (Yoon et al., 2014), the same HACs production process as in the ISM could



occur in the Titan’s upper atmosphere.

But this explanation is not completely satisfactory, mainly because we should find absorptions in the wavelength range 3.38–3.48  $\mu\text{m}$  in high altitude occultation spectra which is not the case (Courtin et al., 2015). In this latter reference, the authors do not observe strong features (in extinction) in this wavelength range above 500 km but rather below 480 km (Courtin et al., 2015, Fig. 2). The authors computed the 3.33  $\mu\text{m}$  / 3.38  $\mu\text{m}$  extinction coefficient ratio, the wavelength at 3.33  $\mu\text{m}$  being characteristic of aromatic C–H stretching and the wavelength at 3.38  $\mu\text{m}$  characteristic of aliphatic C–H stretching. Thus, this ratio is function of the ratio between the aromatic and aliphatic components in the haze particles. This ratio is about 3 at 700 km and decreases to about 0.5 below 300 km. Then the conclusion of Courtin et al. (2015) is a growth of molecules from PAHs to more complex organics by particle-aging and coating process when the altitude decreases. So, even if the explanation in Dartois et al. (2004, 2005) about the HACs production in the ISM is not completely relevant for Titan’s upper atmosphere, it is possible to have HACs at low altitude, by particle-aging and coating process. This process was also studied in laboratory by ultraviolet irradiation of analogs of Titan’s thermosphere aerosols (Carrasco et al., 2018; Couturier-Tamburelli et al., 2018). Carrasco et al. (2018) analyzed the absorption peaks of residues and their time evolution. They found shifts and modifications of vibrational signatures reflecting aerosols transformation during the irradiation. The observed spectra after 24 h of irradiation appear to tend toward Titan’s spectra observed in VIMS spectra at altitude 200 km. The conclusion of Carrasco et al. (2018) is that a particle aging process by ultraviolet irradiation occurs in Titan’s atmosphere from aerosol embryos in thermosphere to more complex haze particles in low altitudes according the following process: (1) aerosol embryos generation, (2) sedimentation and (3) chemical evolution by UV irradiation.

Other studies were conducted (Gudipati et al., 2013; Yoon et al., 2014). In Yoon et al. (2014), the authors experimentally studied the role of benzene photolysis in the PAHs and more complex particles (*tholins*) production. They stipulated that UV radiation with wavelengths longer than 130 nm (FUV domain) leads to the photodissociation of benzene. Likewise, in the FUV domain the photons could reach low altitudes bringing a benzene photolysis in the lower atmosphere. Then this photolysis would lead to the production of PAHs and more complex particles. In the same way, Gudipati et al. (2013); Couturier-Tamburelli et al. (2014) proceeded to photochemical experiments with  $\text{C}_4\text{N}_2$  ice and photons in FUV domain, reproducing the environment of Titan’s lower atmosphere and highlighting the fact that at low altitudes (below 200 km) the UV flux at 350 nm is comparable to the upper radiation field at shorter wavelengths. Their conclusion is that photoabsorption by haze particles in this FUV domain would trigger a rich solid-state chemistry at low altitudes. In a similar way photolysis of  $\text{HC}_5\text{N}$  led

to residues containing aromatic signatures around 3.3  $\mu\text{m}$  and C–H stretching around 3.4  $\mu\text{m}$  (Couturier-Tamburelli et al., 2015). The authors concluded that this photolysis drives the formation of more and more complex polymers which are precursors of haze particles. These results about the PAHs and HACs production at low altitudes are in agreement with our spectral analysis of the 3.4  $\mu\text{m}$  band for the occultation at 145 km of altitude.

Finally, NASA has recently announced the selection of the *Dragonfly* mission (Turtle et al., 2019) as part of its *New Frontiers* program. This revolutionary quacopter is planned to explore Titan’s surface, in the region of Shangri-La dune fields and Selk impact crater, during the mid-2030s. Among onboard instruments, the *Dragonfly Camera Suite* will allow PAH detection via fluorescence, excited by a controlled UV illumination (Lorenz et al., 2018).

## 7. Conclusion

To conclude, the present study was to explain the strong absorption around 3.4  $\mu\text{m}$  observed in the occultation spectra by VIMS at low altitudes typically lower than 450 km. We opted for the altitude 145 km which offers a good compromise: at lower altitudes, the stronger absorptions damp spectral features and at higher altitudes, the absorptions are too weak to be extracted from the signal. As a first step in our radiative transfer modeling, we have included 9 molecules following Maltagliati et al. (2015):  $\text{CH}_4$ ,  $\text{CH}_3\text{D}$ ,  $\text{CO}$ ,  $\text{C}_2\text{H}_2$ ,  $\text{C}_2\text{H}_4$ ,  $\text{C}_2\text{H}_6$ ,  $\text{H}_2\text{O}$ ,  $\text{C}_6\text{H}_6$  and  $\text{HCN}$ . This composition leads to a poor reproduction of the observed transmittance curve. The disagreement was reduced by including  $\text{C}_2\text{H}_6$  spectroscopic data as the data coming from Pine and Lafferty (1982) or the more exhaustive data, but empirical pseudo-line, coming from Harrison et al. (2010). This way, the agreement has been improved, but the simulated transmittance remained above the observed one. The inclusion of propane improved the result but there was still a lack of efficient absorbers around 3.4  $\mu\text{m}$ . Knowing that spectral signatures around 3.4  $\mu\text{m}$  are present in the ISM and identified as PAHs or HACs, we have considered these complex hydrocarbon compounds in our model as possible absorbers in the Titan’s atmosphere at about 145 km of altitude. The fit of abundance of PAHs and HACs, taking into account some uncertainty by means of a correction factor, allowed a rather satisfactory modelization of the observed transmittance at 145 km of altitude. Thus, the model suggests the presence of complex hydrocarbon compounds and precursors of haze particles at low altitudes. This result is also consistent with several laboratory studies showing a complexification of hydrogenated molecules from small hydrocarbons to more complex by UV irradiations (Yoon et al., 2014; Couturier-Tamburelli et al., 2015, 2018; Carrasco et al., 2018).

## Acknowledgment

We thank Laurence Regalia, Michael Rey, Bruno Bézard, Walter Lafferty, Christophe Sotin and Jean Vander Auvera for scientific discussion. We are grateful to Christiaan Boersma for his kind technical help in using the NASA Ames PAH database. Finally, we warmly thank Vladimir Krasnopolsky for providing us with vertical profiles of organics.

## Appendix A. Spectral data references

**Table 2:** Summary of spectral line lists used in this study.

Molecules	Lines source
CH <sub>4</sub>	Theoretical Reims-Tomsk Spectral database <sup>a</sup>
CH <sub>3</sub> D	Theoretical Reims-Tomsk Spectral database <sup>a</sup>
CO	HITRAN <sup>b</sup> , GEISA <sup>c</sup>
C <sub>2</sub> H <sub>2</sub>	HITRAN <sup>b</sup> , GEISA <sup>c</sup>
C <sub>2</sub> H <sub>4</sub>	Theoretical Reims-Tomsk Spectral database <sup>a</sup>
C <sub>2</sub> H <sub>6</sub>	HITRAN <sup>b</sup> , PL82 <sup>d</sup> , H10 <sup>e</sup>
H <sub>2</sub> O	HITRAN <sup>b</sup> , GEISA <sup>c</sup>
C <sub>6</sub> H <sub>6</sub>	Ab-initio MP2/6-211**
HCN	HITRAN <sup>b</sup> , GEISA <sup>c</sup>
C <sub>3</sub> H <sub>8</sub>	H10-P <sup>f</sup>
C <sub>4</sub> H <sub>10</sub>	NIST <sup>g</sup>
PAHs	NASA AMES PAHs IR Spectroscopic database <sup>h</sup>
HACs	Dartois et al. (2007)

<sup>a</sup> Rey et al. (2016) - [theorets.tsu.ru](http://theorets.tsu.ru)

<sup>b</sup> Rothman et al. (2013) - [hitran.org](http://hitran.org)

<sup>c</sup> Jacquinet-Husson et al. (2008) - [pole-ether.fr/geisa](http://pole-ether.fr/geisa)

<sup>d</sup> Pine and Lafferty (1982) - Available amount request.

<sup>e</sup> Harrison et al. (2010) - [mark4sun.jpl.nasa.gov/pseudo.html](http://mark4sun.jpl.nasa.gov/pseudo.html)

<sup>f</sup> Harrison and Bernath (2010) - [mark4sun.jpl.nasa.gov/pseudo.html](http://mark4sun.jpl.nasa.gov/pseudo.html)

<sup>g</sup> [webbook.nist.gov](http://webbook.nist.gov)

<sup>h</sup> [astrochem.org/pahdb](http://astrochem.org/pahdb)

## Appendix B. List of VIMS cubes

The list of the VIMS cubes used in the T10E, T53E, T78E and T78I occultations are provided in 4 CSV files. They contain, the cube unique ID (in OPUS format), its folder location on the PDS ([pds-rings.seti.org/holdings/volumes/COVIMS.0xxx/](http://pds-rings.seti.org/holdings/volumes/COVIMS.0xxx/) prefix to get the URL), the cube acquisition start time and the observation sequence name.

## References

Arking A. and Grossman K. [The Influence of Line Shape and Band Structure on Temperatures in Planetary Atmospheres](#). *Journal of the Atmospheric Sciences*, 29(5)937–949, **1972**.

Becker L. and Bunch T. E. [Fullerenes, fullerenes and PAHs in the Allende meteorite](#). *Meteoritics and Planetary Science*, 32, **1997**.

Becker L., Glavin D. P. and Bada J. L. [Polycyclic aromatic hydrocarbons \(PAHs\) in Antarctic Martian meteorites, carbonaceous chondrites, and polar ice](#). *Geochimica et Cosmochimica Acta*, 61 475–481, **1997**.

Bellucci A. and 7 colleagues. [Titan solar occultation observed by Cassini/VIMS: Gas absorption and constraints on aerosol composition](#). *Icarus*, 201(1)198–216, **2009**.

Bézard B., Marten A. and Paubert G. [Detection of Acetonitrile on Titan](#). In *American Astronomical Society, 25th DPS Meeting*, volume 25, p 25.09, **1993**.

Bézard B. and 3 colleagues. [Detection of 13CH<sub>3</sub>D on Titan](#). *Icarus*, 191(1)397–400, **2007**.

Bourgalais J. and 9 colleagues. [Elusive anion growth in Titan’s atmosphere: Low temperature kinetics of the C<sub>3</sub>N- + HC<sub>3</sub>N reaction](#). *Icarus*, 271194–201, **2016**.

Carrasco N. and 4 colleagues. [The evolution of Titan’s high-altitude aerosols under ultraviolet irradiation](#). *Nature Astronomy*, 2(6) 489–494, **2018**.

Charnay B. and 4 colleagues. [Titan’s past and future: 3D modeling of a pure nitrogen atmosphere and geological implications](#). *Icarus*, 241269–279, **2014**.

Chou M. D. and Arking A. [Computation of Infrared Cooling Rates in the Water Vapor Bands](#). *Journal of the Atmospheric Sciences*, 37(4)855–867, **1980**.

Cordier D. [How speed-of-sound measurements could bring constraints on the composition of Titan’s seas](#). *Monthly Notices of the Royal Astronomical Society*, 4592008–2013, **2016**.

Cordier D. and 7 colleagues. [Structure of Titan’s evaporites](#). *Icarus*, 27041–56, **2016**.

Courtin R., Kim S. J. and Bar-Nun A. [Three-micron extinction of the Titan haze in the 250–700 km altitude range: Possible evidence of a particle-aging process](#). *Astronomy & Astrophysics*, 573A21, **2015**.

Coustonis A. and 8 colleagues. [Evidence for water vapor in Titan’s atmosphere from ISO/SWS data](#). *Astronomy and Astrophysics*, 336L85–L89, **1998**.

Coustonis A. and 9 colleagues. [Titan’s temporal evolution in stratospheric trace gases near the poles](#). *Icarus*, 270409–420, **2016**.

Couturier-Tamburelli I. and 4 colleagues. [Spectroscopic studies of non-volatile residue formed by photochemistry of solid C<sub>4</sub>N<sub>2</sub>: A model of condensed aerosol formation on Titan](#). *Icarus*, 23481–90, **2014**.

Couturier-Tamburelli I., Piétri N. and Gudipati M. S. [Simulation of Titan’s atmospheric photochemistry. Formation of non-volatile residue from polar nitrile ices](#). *Astronomy and Astrophysics*, 578 A111, **2015**.

Couturier-Tamburelli I. and 4 colleagues. [UV-Vis Light-induced Aging of Titan’s Haze and Ice](#). *The Astrophysical Journal*, 852(2) 117, **2018**.

Cruikshank D. P. and 26 colleagues. [Hydrocarbons on Saturn’s satellites Iapetus and Phoebe](#). *Icarus*, 193334–343, **2008**.

Cui J. and 12 colleagues. [Analysis of Titan’s neutral upper atmosphere from Cassini Ion Neutral Mass Spectrometer measurements](#). *Icarus*, 200581–615, **2009**.

Dartois E. and 3 colleagues. [Diffuse interstellar medium organic polymers. Photoproduction of the 3.4, 6.85 and 7.25 Mm features](#). *Astronomy and Astrophysics*, 423L33–L36, **2004**.

Dartois E. and 4 colleagues. [Ultraviolet photoproduction of ISM dust. Laboratory characterisation and astrophysical relevance](#). *Astronomy and Astrophysics*, 432895–908, **2005**.

Dartois E. and 8 colleagues. [IRAS 08572+3915: Constraining the aromatic versus aliphatic content of interstellar HACs](#). *Astronomy & Astrophysics*, 463(2)635–640, **2007**.

Dinelli B. M. and 6 colleagues. [An unidentified emission in Titan’s upper atmosphere](#). *Geophysical Research Letters*, 401489–1493, **2013**.

Flasar M. and 44 colleagues. [Titan’s Atmospheric Temperatures, Winds, and Composition](#). *Science*, 308(5724)975–978, **2005**.

Fu Q. and Liou K. N. [On the Correlated k-Distribution Method for Radiative Transfer in Nonhomogeneous Atmospheres](#). *Journal of the Atmospheric Sciences*, 49(22)2139–2156, **1992**.

Fulchignoni M. and 42 colleagues. [In situ measurements of the physical characteristics of Titan’s environment](#). *Nature*, 438(7069)785–791, **2005**.

Gross J. and Sadowski G. [Perturbed-Chain SAFT: An Equation of State Based on a Perturbation Theory for Chain Molecules](#). *Industrial & Engineering Chemistry Research*, 40(4)1244–1260, **2001**.

- Gudipati M. S. and 4 colleagues. Photochemical activity of Titan's low-altitude condensed haze. *Nature Communications*, 4(1)1–8, **2013**.
- Guerlet S. and 5 colleagues. Stratospheric benzene and hydrocarbon aerosols detected in Saturn's auroral regions. *Astronomy and Astrophysics*, 580A89, **2015**.
- Harrison J. J. and Bernath P. F. Infrared absorption cross sections for propane (C<sub>3</sub>H<sub>8</sub>) in the 3  $\mu$ m region. *Journal of Quantitative Spectroscopy and Radiative Transfer*, 111(9)1282–1288, **2010**.
- Harrison J. J., Allen N. D. C. and Bernath P. F. Infrared absorption cross sections for ethane (C<sub>2</sub>H<sub>6</sub>) in the 3  $\mu$ m region. *Journal of Quantitative Spectroscopy and Radiative Transfer*, 111(3)357–363, **2010**.
- Jacquinet-Husson N. and 52 colleagues. The GEISA spectroscopic database: Current and future archive for Earth and planetary atmosphere studies. *Journal of Quantitative Spectroscopy and Radiative Transfer*, 1091043–1059, **2008**.
- Johnson R. E., Tucker O. J. and Volkov A. N. Evolution of an early Titan atmosphere. *Icarus*, 271202–206, **2016**.
- Kim S. J. and 5 colleagues. The three-micron spectral feature of the Saturnian haze: Implications for the haze composition and formation process. *Planetary and Space Science*, 65122–129, **2012**.
- Kim S. J. and 7 colleagues. Retrieval and tentative identification of the 3  $\mu$ m spectral feature in Titan's haze. *Planetary and Space Science*, 59699–704, **2011**.
- Koskinen T. T. and 7 colleagues. The mesosphere and lower thermosphere of Titan revealed by Cassini/UVIS stellar occultations. *Icarus*, 216(2)507–534, **2011**.
- Krasnopolsky V. A. A photochemical model of Titan's atmosphere and ionosphere. *Icarus*, 201226–256, **2009**.
- Krasnopolsky V. A. The photochemical model of Titan's atmosphere and ionosphere: A version without hydrodynamic escape. *Planetary and Space Science*, 581507–1515, **2010**.
- Krasnopolsky V. A. Chemical composition of Titan's atmosphere and ionosphere: Observations and the photochemical model. *Icarus*, 23683–91, **2014**.
- Lara L. M. and 3 colleagues. Vertical distribution of Titan's atmospheric neutral constituents. *Journal of Geophysical Research*, 10123261–23283, **1996**.
- Lavvas P. and 6 colleagues. N<sub>2</sub> state population in Titan's atmosphere. *Icarus*, 26029–59, **2015**.
- Lavvas P., Coustenis A. and Vardavas I. M. Coupling photochemistry with haze formation in Titan's atmosphere, Part I: Model description. *Planet. Space Sci.*, 56(1)27–66, **2008a**.
- Lavvas P., Coustenis A. and Vardavas I. M. Coupling photochemistry with haze formation in Titan's atmosphere, Part II: Results and validation with Cassini/Huygens data. *Planet. Space Sci.*, 56(1) 67–99, **2008b**.
- Lavvas P. and 3 colleagues. Surface chemistry and particle shape: Processes for the evolution of aerosols in Titan's atmosphere. *Astrophys. J.*, 728(2)80, **2011**.
- Li A. PAHs in Comets: An Overview. In Käuffel H. and Sterken C., editors, *Deep Impact as a World Observatory Event: Synergies in Space, Time, and Wavelength*, Eso Astrophysics Symposia, pp 161–175, Berlin, Heidelberg, **2009**. Springer.
- López-Puertas M. and 8 colleagues. Large Abundances of Polycyclic Aromatic Hydrocarbons in Titan's Upper Atmosphere. *The Astrophysical Journal*, 770132, **2013**.
- Lorenz R. D. and 16 colleagues. Dragonfly: A Rotorcraft Lander Concept for Scientific Exploration at Titan. Johns Hopkins APL, **2018**.
- Luspay-Kuti A. and 6 colleagues. Experimental constraints on the composition and dynamics of Titan's polar lakes. *Earth and Planetary Science Letters*, 41075–83, **2015**.
- Magee B. A. and 5 colleagues. INMS-derived composition of Titan's upper atmosphere: Analysis methods and model comparison. *Planetary and Space Science*, 571895–1916, **2009**.
- Maltagliati L. and 8 colleagues. Titan's atmosphere as observed by Cassini/VIMS solar occultations: CH<sub>4</sub>, CO and evidence for C<sub>2</sub>H<sub>6</sub> absorption. *Icarus*, 2481–24, **2015**.
- Møller C. and Plesset M. S. Note on an Approximation Treatment for Many-Electron Systems. *Physical Review*, 46618–622, **1934**.
- Müller-Wodarg I. and 3 colleagues. Titan : Interior, surface, atmosphere, and space environment, **2013**.
- Newman C. E. and 3 colleagues. Simulating Titan's methane cycle with the TitanWRF General Circulation Model. *Icarus*, 267106–134, **2016**.
- Nicholson P. D. and 3 colleagues. Probing Saturn's Atmosphere with Procyon. In *American Astronomical Society, 38th DPS Meeting*, **2006**.
- Nixon C. A. and 11 colleagues. Detection of Propene in Titan's Stratosphere. *The Astrophysical Journal Letters*, 776L14, **2013**.
- Pendleton Y. J. and Allamandola L. J. The Organic Refractory Material in the Diffuse Interstellar Medium: Mid-Infrared Spectroscopic Constraints. *The Astrophysical Journal Supplement Series*, 13875–98, **2002**.
- Pine A. and Lafferty W. Torsional Splittings and Assignments of the Doppler-Limited Spectrum of Ethane in the C-H Stretching Region. *Journal of Research of the National Bureau of Standards*, 87(3)237, **1982**.
- Poling B. E., Prausnitz J. M. and O'Connell J. P. *Properties of Gases and Liquids*. McGraw-Hill Professional, Englewood Cliffs, 5th edition, **2007**.
- Rey M. and 3 colleagues. TheoReTS - An information system for theoretical spectra based on variational predictions from molecular potential energy and dipole moment surfaces. *Journal of Molecular Spectroscopy*, 327138–158, **2016**.
- Romanzin C. and 6 colleagues. An experimental study of the reactivity of CN- and C<sub>3</sub>N- anions with cyanoacetylene (HC<sub>3</sub>N). *Icarus*, 268242–252, **2016**.
- Rothman L. S. and 48 colleagues. The HITRAN2012 molecular spectroscopic database. *Journal of Quantitative Spectroscopy and Radiative Transfer*, 1304–50, **2013**.
- Sandford S. A. and 5 colleagues. The interstellar C-H stretching band near 3.4 microns - Constraints on the composition of organic material in the diffuse interstellar medium. *The Astrophysical Journal*, 371607–620, **1991**.
- Sharpe S. W. and 5 colleagues. Gas-Phase Databases for Quantitative Infrared Spectroscopy. *Applied Spectroscopy*, **2016**.
- Tan S. P., Kargel J. S. and Marion G. M. Titan's atmosphere and surface liquid: New calculation using Statistical Associating Fluid Theory. *Icarus*, 222(1)53–72, **2013**.
- Tan S. P. and 5 colleagues. Titan's liquids: Exotic behavior and its implications on global fluid circulation. *Icarus*, 25064–75, **2015**.
- Turtle E. P. and 44 colleagues. Dragonfly: In Situ Exploration of Titan's Organic Chemistry and Habitability. In *50th Lunar and Planetary Science Conference*, volume 50, p 2888, **2019**.
- Vinater S. and 10 colleagues. Analysis of Cassini/CIRS limb spectra of Titan acquired during the nominal mission: I. Hydrocarbons, nitriles and CO<sub>2</sub> vertical mixing ratio profiles. *Icarus*, 205(2)559–570, **2010**.
- Vinater S. and 10 colleagues. Seasonal variations in Titan's middle atmosphere during the northern spring derived from Cassini/CIRS observations. *Icarus*, 25095–115, **2015**.
- Yoon Y. H. and 5 colleagues. The role of benzene photolysis in Titan haze formation. *Icarus*, 233233–241, **2014**.